LHCb-INT-2011-013
April 19, 2011

Study of the 2010 alignment stability using J/ψ and D^0 decays

Yasmine Amhis[1], Jibo He[2], Raphael Märki[1], Matthew Needham[3] and Olivier Schneider[1]

[1] *Ecole Polytechnique Fédérale de Lausanne (EPFL), Lausanne, Switzerland*
[2] *LAL, Université Paris-Sud, CNRS/IN2P3, Orsay, France*
[3] *School of Physics and Astronomy, University of Edinburgh, Edinburgh, United Kingdom*

Abstract

The stability of the LHCb tracking alignment during the 2010 data-taking period is discussed. Using $J/\psi \to \mu^+\mu^-$ decays, shifts in the measured J/ψ mass are observed and correlated to changes in the operating temperature of the TT detector. To correct for these shifts a new time-dependent alignment procedure has been developed based on $D^0 \to K^-\pi^+$ decays. With this procedure a relative stability of 2×10^{-4} on the reconstructed J/ψ mass is achieved over the full 2010 data-taking period.

Contents

1 Introduction **1**

2 TT temperature variation **1**

3 Software alignment procedures **4**
3.1 Global alignment 4
3.2 New alignment procedure based on the D^0 mass constraint 4

4 Validation with resonances **7**

5 Run-dependent alignment **11**
5.1 Residual studies 11
5.2 Mass stability 11

6 Summary **13**

A Calibrated mass values **14**

1 Introduction

To perform precise measurements of particle masses a good alignment of the spectrometer is essential. The standard LHCb alignment procedure makes use of high-momentum tracks ($p > 30$ GeV/c) together with information coming from the vertex and mass constraints for selected $J/\psi \to \mu^+\mu^-$ candidates [1]. This procedure, though adequate, still leaves visible biases on the measured mass of all decay channels. In addition, the alignment was only performed for data taken early in the 2010 run and, as will be shown, is not optimal for the data taken towards the end of the run. In this note, a new alignment procedure based on the vertex and mass constraints of selected $D^0 \to K^-\pi^+$ candidates [1] is presented. This procedure is validated on data taken in the early part of the run and is then applied to data taken later in the run.

This note is arranged as follows. First, the variation of the TT operating temperature over the 2010 run period and its impact on the measured J/ψ mass is discussed. Next the D^0 alignment procedure is described and validated using data from early in the 2010 run. Finally, this procedure is applied to the periods when the TT operating temperature changed.

2 TT temperature variation

To minimize the effect of radiation damage it is foreseen to operate the TT detector at a temperature of approximately $0\,^o$C. To achieve this the detector cooling plant must be operated at approximately $-10\,^o$C. For the first part of the 2010 data-taking, the accumulated radiation dose was low and the TT cooling plant was operated at $5\,^o$C. During the later part of the run, as the luminosity increased, frequent high-voltage trips were observed in the detector. To understand the dependence of these trips on the operating temperature towards the end of 2010 the TT detector was cooled down and operated at $-15\,^o$C for several days. As the number of high-voltage trips increased at this lower temperature and other problems developed, it was subsequently decided to warm up the detector first to $-5\,^o$C and then to $5\,^o$C.

A posteriori, it is trivial to see that the TT temperature changes have a large effect on the detector alignment and consequently on the measured J/ψ mass. The TT modules are mounted on an aluminium cooling plate which has a thermal coefficient of expansion of $\sim 20 \times 10^{-6}/\,^o$C. The temperature change from $+5\,^o$C to $-15\,^o$C will lead to a contraction of the cooling plate and hence movements of the modules of up to ~ 400 μm [2]. Such a change is large compared to the intrinsic resolution of the detector of up to 50 μm.

The stability of the measured J/ψ mass has been studied for the complete 2010 dataset using the selection criteria and fit procedure given in Ref. [2]. In Fig. 1 (top) the measured J/ψ mass is displayed as a function of the run number. For the early runs the J/ψ mass

[1] Unless specified otherwise, charge-conjugate modes are always implied and, in the case of D^0 decays, no attempt is made to separate the Cabibbo-favoured mode from the doubly Cabibbo-suppressed mode.

[2] The exact size of the movement depends on the mechanical mounting of the cooling plates holding the detector modules.

First run	Last run	Fraction of integr. lumi.	ΔM [MeV/c^2]	TT temperature [^{o}C]
–	81309	53%	1.5	+5
81310	81375	20%	3.3	−15
81376	81476	10%	2.7	−5
81476	–	17%	2.1	+5

Table 1: Bias on the J/ψ mass, ΔM, for the four data-taking periods in 2010 corresponding to different TT temperatures. The alignment v4.2 is used, which was determined with data from the first period. As can be seen the J/ψ constraint in the alignment does not lead to a measured J/ψ mass equal to the PDG value ($\Delta M = 0$) for the first period. Presumably this is due to the fact that tracks other than those coming from the J/ψ decay are used in the alignment, or to the inability of the alignment procedure to correct for biases in the magnetic field map.

is extremely stable over time. However, three steps can be clearly seen. These correspond to the periods in time when the TT operating temperature was changed as discussed above. The first change in TT operating temperature to $-15\,^o$C is so large that it also leads to a noticeable degradation in the J/ψ mass resolution, as shown in Fig. 1 (bottom). The reasons for this have been studied in detail. Figure 2 shows the J/ψ mass for this data-taking period as a function of the angle between the normal to the decay plane and the main component of the magnetic field, ϕ_d, which is known to be a sensitive variable for identifying problems related to the alignment. There is a 10 MeV/c^2 variation of the J/ψ mass as a function of this angle which largely explains the observed degradation of the mass resolution. It is clear that in this case the temperature variation is so large that a full internal and global re-alignment of the TT station is needed.

The average bias on the J/ψ mass, i.e. the difference between the measured J/ψ mass and the PDG value, is given in Table 1 as a function of the data-taking period. When the TT temperature returned to $5\,^o$C the bias on the mass did not return to its initial value. The reason for this is not clear. However, it should be noted that even if the information from the TT station is not used in the determination of the J/ψ mass a small step is seen in the J/ψ mass around the time when TT was first cooled (see top of Fig. 3). Therefore, it is likely that there is a change in the alignment of one of the other tracking detectors that has not yet been accounted for. For completeness Fig. 3 (bottom) shows the J/ψ mass resolution without using the TT information over the entire 2010 run. No significant variation is seen.

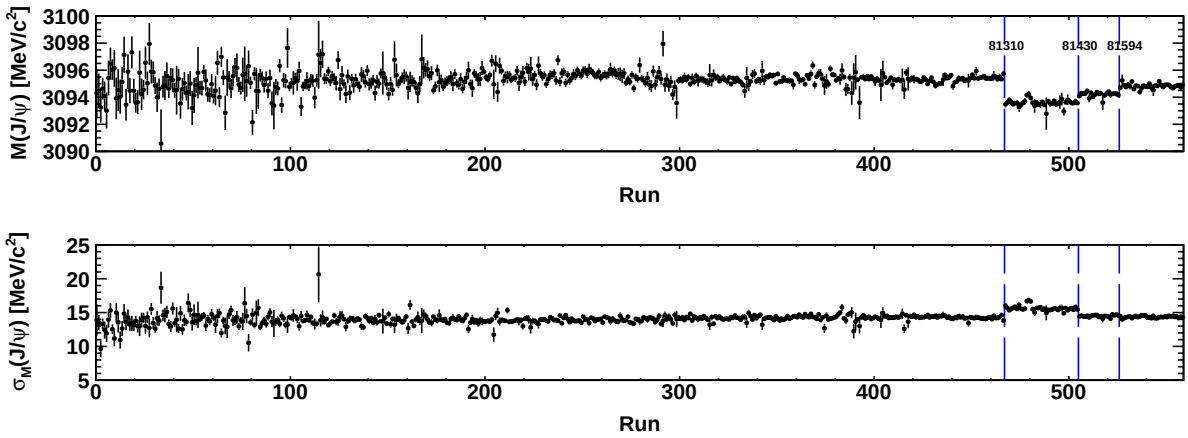

Figure 1: Measured $J/\psi \to \mu^+\mu^-$ mass (top) and resolution (bottom) as a function of run number during the entire 2010 data-taking period. The steps (indicated with vertical lines) correspond to the times when the TT operating temperature was altered.

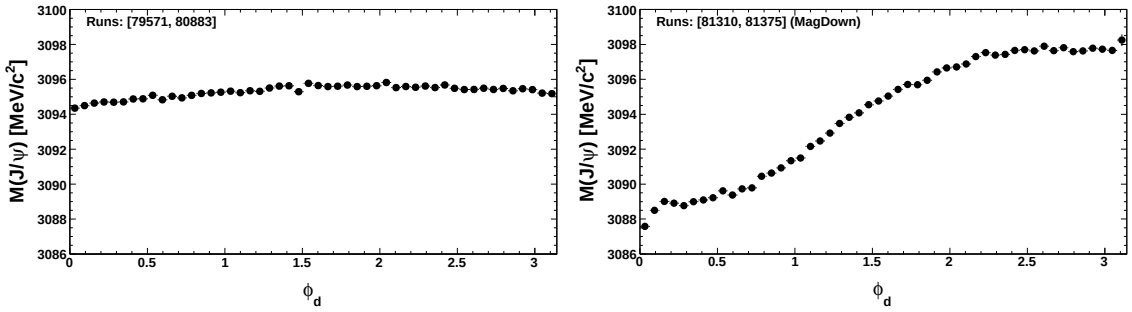

Figure 2: Measured J/ψ mass as a function of the angle ϕ_d for the data taken early in the run when TT was at $+5\,^o$C (left) and the later period when the TT operating temperature was $-15\,^o$C (right).

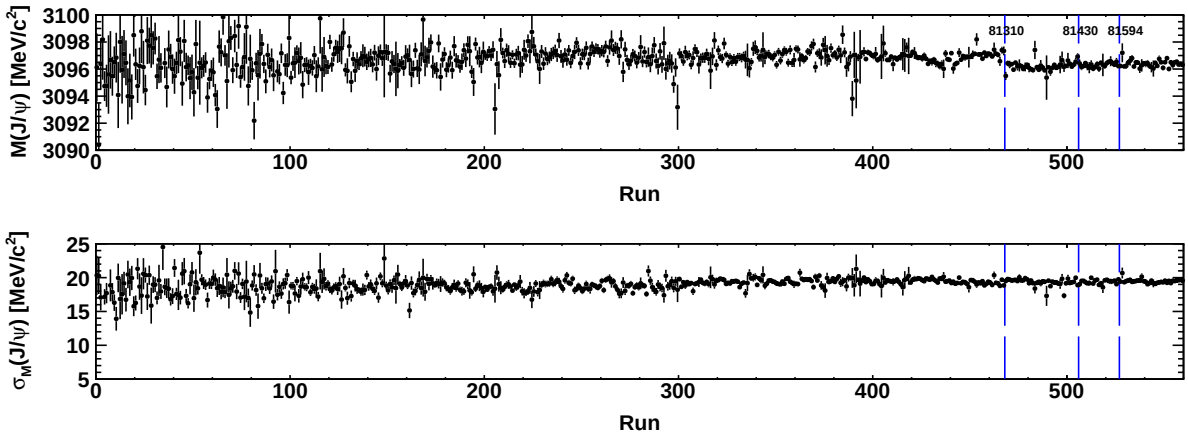

Figure 3: Measured $J/\psi \to \mu^+\mu^-$ mass (top) and J/ψ mass resolution (bottom) as a function of run number during the entire 2010 data-taking, when the information from the TT station is ignored.

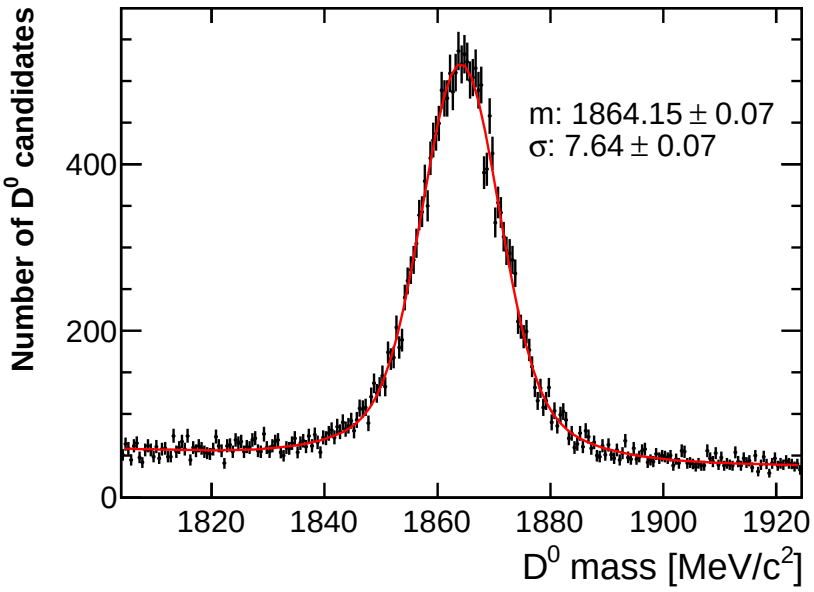

Figure 4: Fitted $D^0 \to K^-\pi+$ mass distribution in the used data sample. As can be seen the signal-to-background ratio is high.

3 Software alignment procedures

3.1 Global alignment

The procedure for the global alignment of the LHCb detector is described in Ref. [3]. A closed form Kalman filter method is used which correctly takes account the correlations between the track parameters and the detector components that are being aligned.

From previous studies [4] it is known that for the alignment to converge to the global minimum care is needed both in the choice of the parameters to be aligned for and in the track selection to remove poorly reconstructed tracks. If the tracks and the free alignment parameters are well chosen, the procedure converges to a minimum value of the χ^2 after a few iterations. A powerful way to select good tracks is to use the tracks from the decay $J/\psi \to \mu^+\mu^-$ and make use of the vertex and mass constraints that this channel provides. This is the approach adopted in the currently used alignment [1].

3.2 New alignment procedure based on the D^0 mass constraint

A new alignment method was developed to constrain the two tracks from $D^0 \to K^-\pi^+$ candidates to form a common vertex and have an invariant mass equal to the PDG value. This approach has several advantages compared to the alignment based on $J/\psi \to \mu^+\mu^-$ candidates. First, the D^0 signal is clean (see Fig. 4) and hence the procedure is less sensitive to background. In addition, the decay kinematics are different. Due to the fact

	IT overlap tracks	High-momentum IT tracks	Tracks with many VELO hits
RequireOverlap	True	—	—
MinPCut	30 GeV/c	50 GeV/c	—
MaxPCut	200 GeV/c	200 GeV/c	—
MaxEtaCut	4.6	4.6	—
MaxChi2Cut	5	5	5
MaxChi2PerDoFMatch	5	5	5
MaxChi2PerDoFVelo	5	5	5
TrackTypes	Long	Long	Long
MinNITHits	4	8	—
MinNVeloRHits	5	5	13
MinNVeloPhiHits	5	5	13

Table 2: Track selection for IT overlap tracks, high-momentum IT tracks, and tracks with many VELO hits.

that $M_K > M_\pi$ the momentum asymmetry between the daughters particles is larger than in the J/ψ case.

As a first check the alignment procedure is validated using data from the first data-taking period in Table 1. D^0 candidates are selected from a charm stripping line (D02hhPIDLine) within a ± 24 MeV/c^2 ($\pm 3\sigma$) mass window around the known mass of the D^0. The tracks of their daughter particles are then refitted so as to constrain them to come from a common decay vertex and to reproduce the known D^0 mass. A contribution to the χ^2 of the alignment is then given based on the new residuals of the daughter tracks taking into account the correlation between them introduced by the vertex and mass constraint.

Additional tracks are needed by the alignment procedure to increase the statistics and provide enough constraints. Tracks falling in any of the following categories are selected in the events containing the D^0 candidates:

- Tracks passing through the overlap regions of two IT boxes or the overlap regions between IT and OT;
- High momentum IT tracks;
- Tracks with many VeLo hits.

The selection requirements applied for each category are listed in Table 2. All tracks in the considered D^0 events that satisfy these requirements are used in the alignment procedure. In this procedure it was chosen to align for the same degrees of freedom as in the v4.2 alignment, listed in Table 3.

For 100'000 events of the considered D^0 stripping line, approximately 120'000 tracks from D^0 candidates and 180'000 additional tracks are selected for use in the alignment.

Element	Degree of freedom
ITBoxes	Tx Tz Rz
ITLayers	Tx Tz
ITLadders	Tx Rz
OTCFrames	Tx
OTCFrameLayers	Tz
OTModules	Tx Rz
TT	Tz
TTLayers	Tz
TTModules	Tx Rz

Table 3: List of degrees of freedom used in the D^0 mass constrained alignment procedure. Tx, Tz and Rz indicate translation along x axis, translation along z axis, and rotation around z axis, respectively.

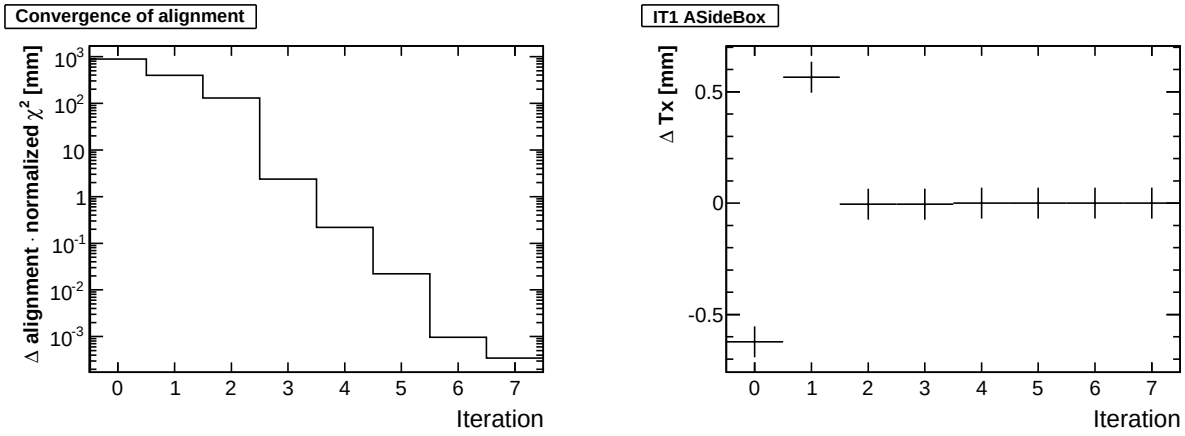

Figure 5: Left: evolution (as a function of iteration number) of the total movement times the normalized χ^2 during the new alignment with D^0 mass constraint, showing good convergence of the procedure. Right: translation along the x axis of an IT box at each iteration of the alignment procedure.

The alignment procedure is tested with different data samples from different data taking periods and different starting points (initial alignment conditions). The alignment typically converges in a few iterations (see Fig. 5) and gives similar constants within the statistical precision to those found with the v4.2 alignment. As an example of the quality of the alignment the distribution of unbiased residuals in the TT detector is shown in Fig. 6. Further validation using various decays will be discussed in the next section.

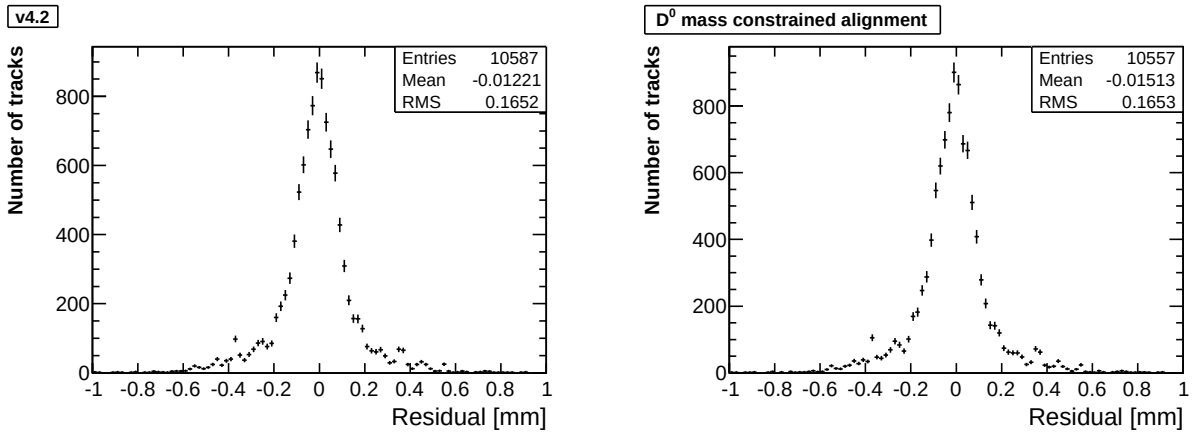

Figure 6: Overlap residuals in TTaX with v4.2 alignment (left) and after alignment performed with the D^0 mass constraint (right). The new residual distribution is as good as the previous one.

4 Validation with resonances

The quality of the new alignment has been validated and compared to the numbers found for the previous version (v4.2) that was used in the **Stripping12** production. As discussed in Ref. [2] two-body decays of resonances provide powerful tests of the validity of an alignment. Detailed studies have been performed using the sample of around 15 pb^{-1} of data in DST format from the inclusive dimuon stream collected with field up polarity discussed in Ref. [2]. This sample belongs to the first period listed in Table 1. To check the new alignment a full refit was performed for the tracks on selected candidates [3]. Details of the selection criteria and fit procedure are given in Ref. [2].

The large number of J/ψ candidates in the data sample allows the reconstructed J/ψ mass to be studied as a function of the momentum difference $p_+ - p_-$, the angle between the normal to the J/ψ decay plane and the orientation of the magnetic field (ϕ_d) and the J/ψ momentum. In addition, as in Ref. [2], the dependence of the J/ψ mass bias on the track pseudo-rapidity (η) has been studied using candidates where the two muons have similar rapidity. In Figs. 7–10 the bias on the J/ψ mass is compared between the v4.2 alignment and the D^0-based alignment for each of the four variables listed above. The average bias on the mass of -1.5 MeV/c^2 is similar for both alignments. However, the variation of the bias across phase space is clearly reduced with the new alignment. This is quantified in Table 4 where the peak-to-peak variation observed for these variables is compared between the two alignments.

The bias has also been studied for other two-body decays with the new alignment. To allow a proper comparison the observed difference between the measured mass and the PDG mass, the mass bias is converted into the equivalent shift of the momentum scale, α, using the procedure discussed in Ref. [2] that correctly takes into account relativistic

[3]The new alignment is included as a slice.

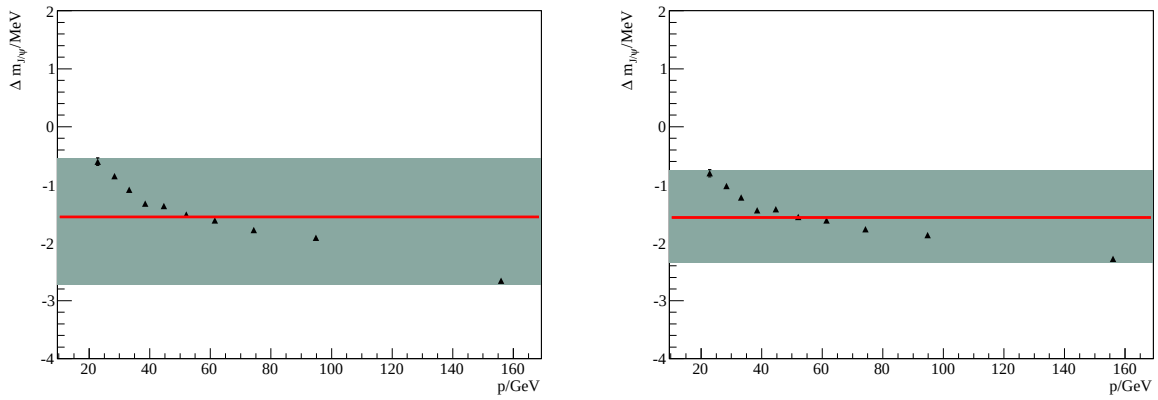

Figure 7: Bias on the reconstructed J/ψ mass as a function of momentum for the v4.2

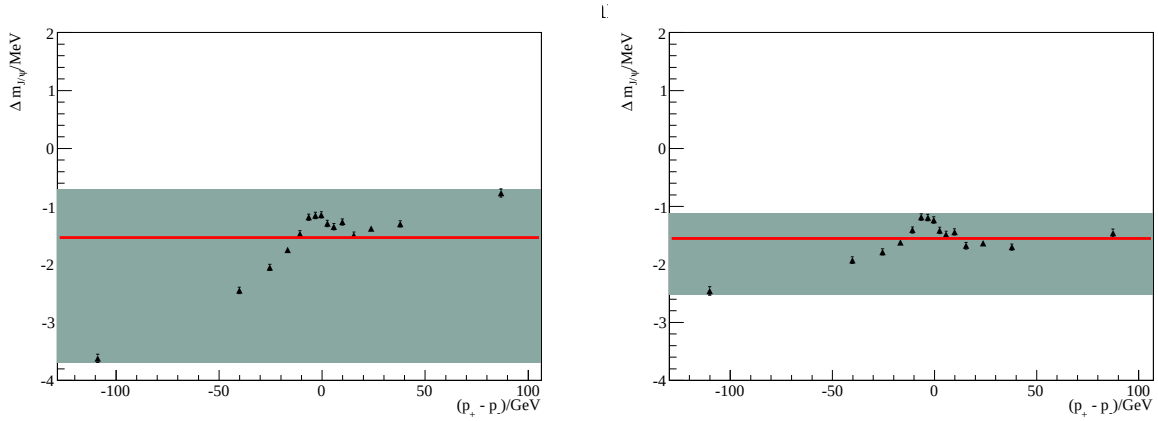

Figure 8: Bias on the reconstructed J/ψ mass as a function of $p_+ - p_-$ for the v4.2 alignment (left) and for the D^0-based alignment (right). The filled area indicates the peak-to-peak variation and the red line the average bias.

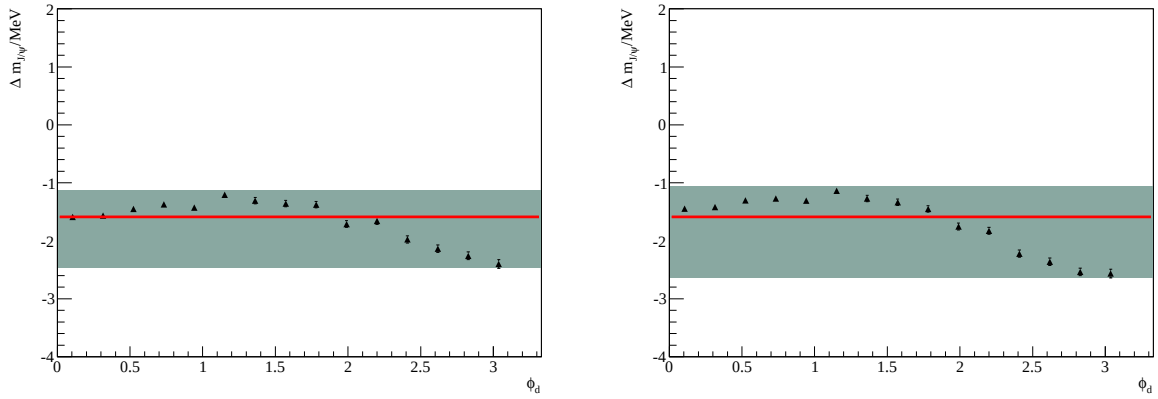

Figure 9: Bias on the reconstructed J/ψ mass as a function of ϕ_d for the v4.2 alignment (left) and for the D^0-based alignment (right). The filled area indicates the peak-to-peak variation and the red line the average bias.

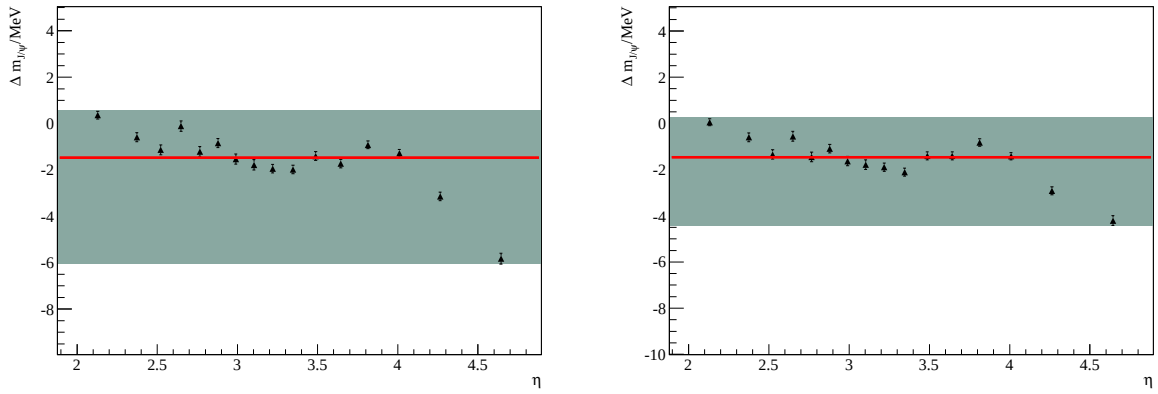

Figure 10: Bias on the J/ψ mass versus η for events where both muons are in the same η bin for alignment v4.2 alignment (left) and the D^0 alignment (right). The filled area indicates the peak-to-peak variation and and the red line the average bias.

Variable	Peak-to-peak bias variation [MeV/c^2]	
	Alignment v4.2	D^0-alignment
p	2.3	1.6
$p_+ - p_-$	3.0	1.4
ϕ_d	1.3	1.6
η	6.2	4.7

Table 4: Peak-to-peak variations of the bias on the reconstructed J/ψ mass for the four test variables with the v4.2 and D^0 based alignment.

kinematics. The results of these studies are summarized in Fig. 11. The momentum scale factors, α, [4] extracted from most of the decays agree at the level of 0.1 per mille. As with the v4.2 alignment there are two exceptions to this: the ϕ and Λ decays. Due to their low Q-values [5] these decays are the least sensitive to the momentum scale and this discrepancy points to the presence of other systematic effects, related to the determination of the opening angle. Two improvements with respect to the previous v4.2 alignment are seen:

- The average of the four Λ measurements, α_Λ, is closer to the average of the other modes. With the v4.2 alignment $\alpha_\Lambda = 1.0$ per mille, whilst with the D^0 alignment $\alpha_\Lambda = 0.5$ per mille.

- The measurements for the Λ and $\overline{\Lambda}$ are more consistent. For example with v4.2

[4] As in Ref. [2], $1 - \alpha$ is the factor that the momentum needs to be corrected by.
[5] Q is the energy released in the decay.

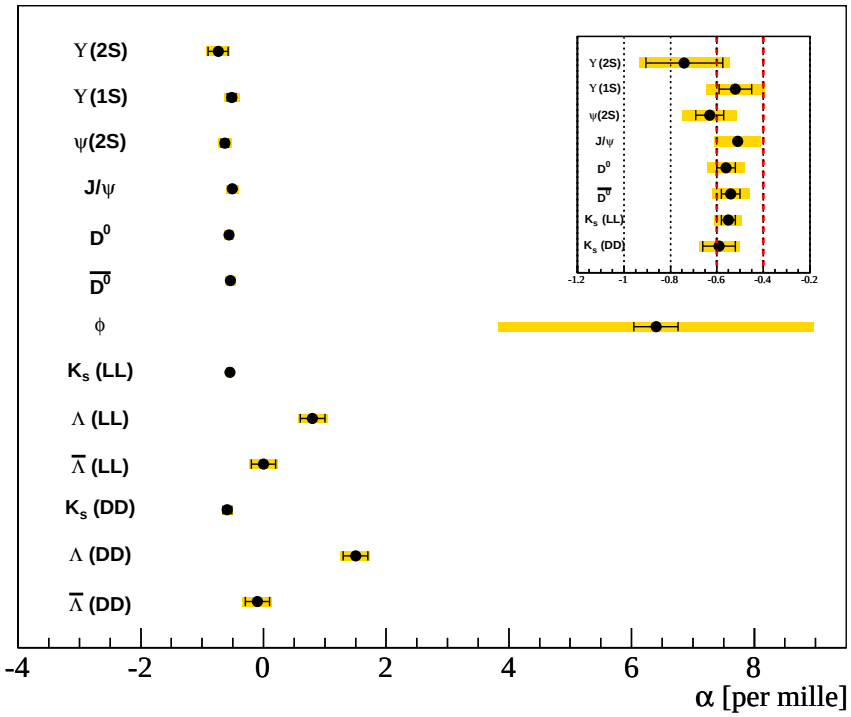

Figure 11: Momentum scale factors extracted from different two-body resonance decays using the D^0-based alignment. The error bars represent the statistical uncertainty whilst the filled area also includes systematic effects as discussed in Ref. [2]. The insert shows a zoom of the region around $\alpha = -0.5$ per mille.

Mode	Resolution [MeV/c^2]	
	Alignment v4.2	D^0 Alignment
$\Upsilon(1S)$	49.31	49.27
J/ψ	14.19	14.17
D^0	7.97	7.93

Table 5: Mass resolution with the v4.2 and D^0-based alignments for some of the two-body modes considered in this study.

$\alpha_{\Lambda(LL)} - \alpha_{\overline{\Lambda}(LL)} = 1.1$ per mille to be compared to 0.8 with the D^0-based alignment.

The mass resolution with the new alignment has been studied for the $\Upsilon(1S) \to \mu^+\mu^-$, $J/\psi \to \mu^+\mu^-$ and $D^0 \to K^-\pi^+$ decay modes. The new alignment improves the mass resolution by $1-2$ MeV/c^2 in quadrature depending on the mode (see Table 5).

TT temperature	$+5\,^{o}$C	$-15\,^{o}$C	$-5\,^{o}$C
Run numbers	75335–77004	81315–81358	81433–81463
Number of events	51'976	100'000	100'000
Used D^0 candidates	30'852	59'984	59'911
Used tracks	91'537	181'637	182'311

Table 6: Data samples used to align for the three different TT temperatures.

5 Run-dependent alignment

The results presented in the previous sections have shown that the new D^0-based alignment gives equivalent or better results than the v4.2 alignment for the early part of the run. To account for the movements in the TT detector observed at the end of the run the procedure has been repeated for the two run periods given in Table 1 where the TT detector was at $-15\,^{o}$C and $-5\,^{o}$C [6]. Since the changes in the alignment are to first order restricted to the TT only the alignment parameters in Table 3 related to this detector are re-evaluated. The data samples used to align for the different periods when TT was at $+5\,^{o}$C, $-15\,^{o}$C and $-5\,^{o}$C are given in Table 6.

5.1 Residual studies

The unbiased residuals in the TT detector with the new alignment have been studied for each of the four periods considered in Table 1. As an example Fig. 12 compares the observed TT overlap residuals for the data-taking period when the TT detector was run at $-15\,^{o}$C for the v4.2 and D^0-based alignments. With the v4.2 alignment procedure the residual distribution shows a bias of 63 μm that is fixed by the new alignment.

5.2 Mass stability

The studies of the J/ψ mass stability described in Section 2 have been repeated with the new alignment. Figure 13 shows the stability of the measured J/ψ mass and resolution over the entire 2010 run. The steps observed earlier have been reduced and the resolution is now constant over the entire running period. The variation of the J/ψ mass as a function of the decay plane angle is also reduced (see Fig. 14). Table 7 summarizes the bias on the J/ψ over the 2010 run. It can be seen that when the TT was warmed again to $+5\,^{o}$C at the end of the run the bias does not return to its original value. The size of the difference is consistent with the value found if the TT information is removed from the track fit. Therefore, it is concluded that this difference is unrelated to the TT detector.

The values in Table 7 were converted to estimates of the momentum scale and used to correct the momenta of the reconstructed tracks in $J/\psi \to \mu^+\mu^-$ candidates. Figure

[6] Since in the last run period the TT detector returns to $+5\,^{o}$C there is, *a priori*, no reason to re-align in this case.

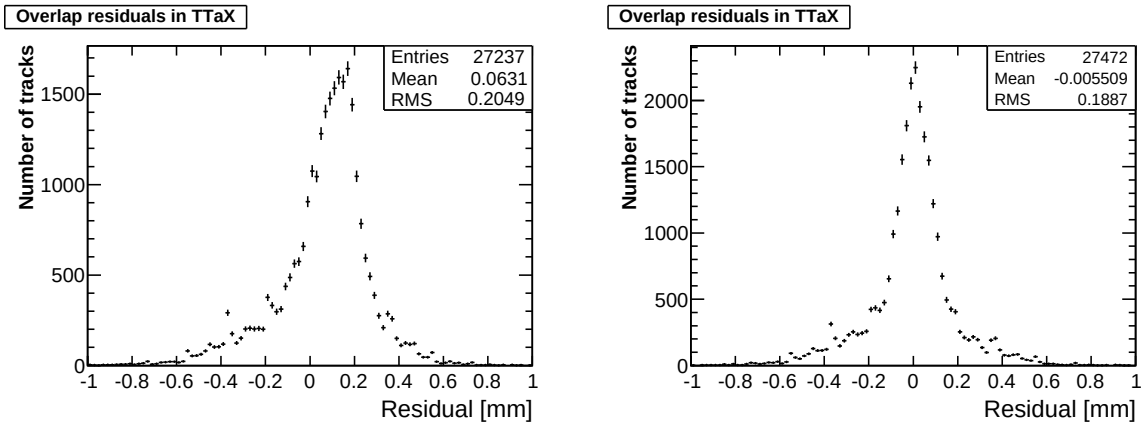

Figure 12: Overlap residuals in TTaX for data taken in the period where TT was at $-15\,^o$C. Alignment v4.2 (left) shows a bias of 63 μm whereas the D^0 based alignment corresponding to this period (right) has a residual distribution centered around zero.

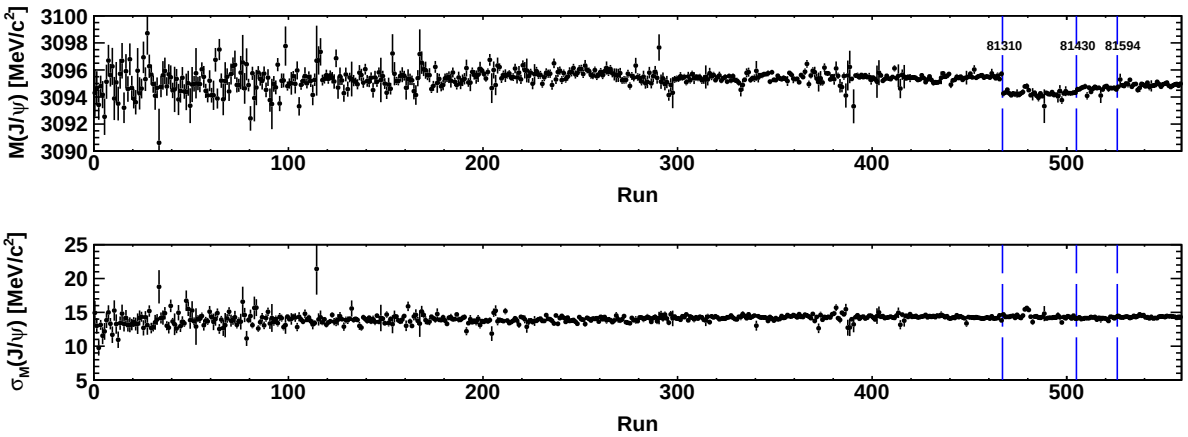

Figure 13: Measured $J/\psi \to \mu^+\mu^-$ mass (top) and resolution (bottom) as a function of run number after the new alignment has been applied. The vertical lines indicate the times when the TT operating temperature was altered.

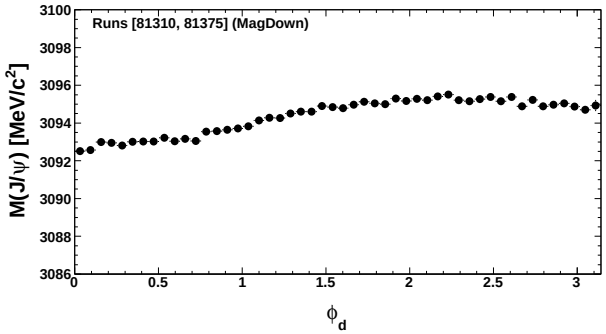

Figure 14: Measured J/ψ mass as function of the angle ϕ_d for the data-taking period when the TT operating temperature was at $-15\,^o$C after the new alignment has been applied.

First run	Last run	ΔM [MeV/c^2]	TT temperature [^{o}C]
–	81310	1.5	+5
81309	81375	2.7	−15
81376	81476	2.3	−5
81476	–	2.0	+5

Table 7: Bias on the measured J/ψ for the different data-taking periods after the D^0-based alignment discussed in the text.

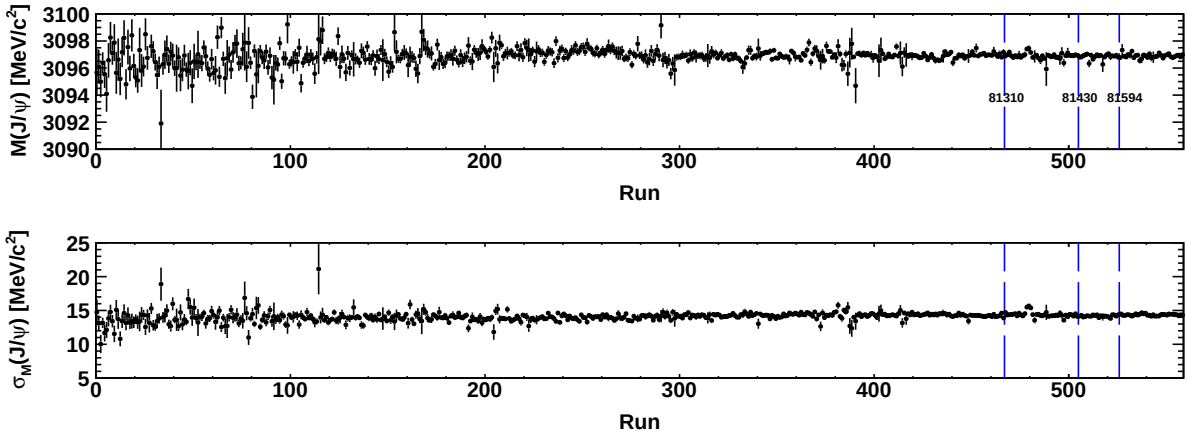

Figure 15: Measured $J/\psi \to \mu^+\mu^-$ mass (top) and resolution (bottom) as a function of run number after the new alignment and momentum scale calibration have been applied. The vertical lines indicate the times when the TT operating temperature was altered.

15 shows the J/ψ mass and resolution after the calibration procedure as a function of the run number. Both the mass and resolution are stable over the entire run.

6 Summary

In this note the stability of the J/ψ mass and resolution over the entire 2010 run period has been studied. Sizeable shifts in the mass are seen towards the end of the run period which are correlated to known changes in the operating temperature of the TT detector.

To correct for these variations a new alignment that uses the mass and vertex constraint provided by $D^0 \to K^-\pi^+$ decays has been developed. This alignment procedure has been validated using other resonance decays and then used to provide alignment constants for each temperature setting of the TT detector. Using this alignment the J/ψ mass is stable at the level of over 0.6 MeV/c^2 over entire 2010 run. This alignment is used as input to the studies of the $X(3872)$ [5] and b-hadron masses [6] that are being performed with the 2010 data.

A Calibrated mass values

Table 8 shows the mass found for two-body resonances after applying the calibration procedure discussed in the text.

Mode	Measured Mass [MeV/c^2]	PDG Mass [MeV/c^2]
$\Upsilon \to \mu^+\mu-$	9459.90 ± 0.54	9460.30 ± 0.26
$J/\psi \to \mu^+\mu-$	3096.97 ± 0.01	3096.916 ± 0.011
$\psi(2S) \to \mu^+\mu-$	3685.72 ± 0.23	3686.09 ± 0.04
$D^0 \to K^-\pi^+$	1864.75 ± 0.07	1864.83 ± 0.14
$\phi \to K^+K^-$	1019.73 ± 0.01	1019.455 ± 0.02
$\Lambda \to p^+\pi^-$	1115.74 ± 0.003	1115.683 ± 0.006
$K^0_s \to \pi^+\pi^-$	497.62 ± 0.01	497.61 ± 0.02

Table 8: Masses of two-body resonance decays after the momentum scale scale calibration procedure. The errors given are statistical only. Systematics errors are not quoted and are expected to larger than the statistical errors.

References

[1] W. Hurslbergen. Update on alignment with J/ψ. Presentation at LHCb Tracking and Alignment meeting on September 2, 2010: `http://indico.cern.ch/contributionDisplay.py?confId=102193`.

[2] M. Needham. Momentum scale calibration with first LHCb data. LHCb-INT-2011-012, 2011.

[3] L. Nicolas *et al.* Alignment of LHCb tracking stations with tracks fitted with a Kalman filter. LHCb-2008-066. In *IEEE Nuclear Science Symposium conference record, N02-3*, pages 1714–1719, 2008.

[4] L. Nicolas *et al.* First Studies of T-station alignment with simulated data. LHCb-PUB-2009-012.

[5] J. Bressieux *et al*. Measurement of the $X(3872)$ mass using 2010 data. LHCb-2011-ANA-030, 2011.

[6] Y. Amhis *et al*. Measurement of b-hadron masses with exclusive $J/\psi X$ decays in 2010 data. LHCb-2011-ANA-027, 2011.